Palaeogeography, Palaeoclimatology, Palaeoecology 574 (2021) 110451

Contents lists available at ScienceDirect

Palaeogeography, Palaeoclimatology, Palaeoecology

journal homepage: www.elsevier.com/locate/palaeo

Analyzing sources of uncertainty in terrestrial organic carbon isotope data: A case study across the K-Pg boundary in Montana, USA

Thomas S. Tobin [a,*], Jacob W. Honeck [a], Isabel M. Fendley [b], Lucas N. Weaver [c], Courtney J. Sprain [b,d], Michael L. Tuite [e], David T. Flannery [e,f], Wade W. Mans [g], Gregory P. Wilson Mantilla [c]

[a] Department of Geological Sciences, University of Alabama, Tuscaloosa, AL 35487, USA
[b] Department of Earth and Planetary Science, University of California, Berkeley, Berkeley, CA 94720, USA
[c] Department of Biology, University of Washington, Seattle, WA 98195, USA
[d] Department of Geological Sciences, University of Florida, Gainesville, FL 32611, USA
[e] Jet Propulsion Laboratory, California Institute of Technology, Pasadena, CA, USA
[f] School of Earth & Atmospheric Sciences, Queensland University of Technology, Brisbane, QLD, Australia
[g] Department of Earth and Planetary Sciences, University of New Mexico, Albuquerque, NM 87131, USA

ARTICLE INFO

Editor: Isabel Montanez

Keywords:
δ13C
Hell Creek
Chemostratigraphy
Cretaceous
Paleogene
Extinction

ABSTRACT

The Cretaceous-Paleogene boundary (KPB) in the Hell Creek area of Montana is recognized in several places by an iridium anomaly, which is typically identified at or very near the lithological contact between the Hell Creek Formation and the Tullock Member of the Fort Union Formation. Previous work in the area has argued that organic carbon isotope ($\delta^{13}C_{org}$) excursions can be used for chemostratigraphic correlation within these continental depositional environments, most importantly for the identification of the KPB where impact evidence is unavailable. However, it is unclear how modern surficial weathering affects $\delta^{13}C_{org}$ values, particularly in terrestrial depositional settings, and whether standard sampling methods are sufficient to obtain unaltered rock material. We tested the fidelity of the terrestrial $\delta^{13}C_{org}$ record with respect to surficial alteration and contamination through investigation of different field sampling techniques, including hand trenches, a backhoe-excavated trench, and sediment coring. We find that $\delta^{13}C_{org}$ values in hand and backhoe trenched sections are more positive than $\delta^{13}C_{org}$ values in cored sections, implying that modern surficial alteration affects $\delta^{13}C_{org}$ values but not overall trends. A negative $\delta^{13}C_{org}$ excursion associated with the KPB is present in most sections we analyzed, but it does not appear to be unique within our sections. The KPB excursion occurs within a coal layer, and we observe similar excursions within other carbon-rich lithologies. Given that we cannot disentangle local lithological effects from global atmospheric changes, we conclude that a negative $\delta^{13}C_{org}$ excursion is not an unequivocal indicator of the KPB in the Hell Creek area.

1. Introduction

1.1. Background

Many major events in Earth history, including mass extinctions and ocean anoxic events, are marked by significant changes to the carbon cycle that can be recognized and characterized by shifts in the carbon isotope ratios ($\delta^{13}C$) of a variety of organic and inorganic carbon reservoirs. These shifts, often dubbed carbon isotope excursions, can be used to correlate these events across the globe, particularly in the marine realm (e.g., Saltzman and Thomas, 2012). Additionally, the magnitude or direction of the $\delta^{13}C$ excursions can reveal information about the nature of global carbon cycle changes. However, the greater spatial heterogeneity of continental environments compared to marine realms raises questions as to whether variability in continental $\delta^{13}C$ records is necessarily driven by changes in atmospheric carbon isotope

* Corresponding author.
E-mail addresses: ttobin@ua.edu (T.S. Tobin), jwhoneck@crimson.ua.edu (J.W. Honeck), isabel.fendley@berkeley.edu (I.M. Fendley), lukeweav@uw.edu (L.N. Weaver), csprain@ufl.edu (C.J. Sprain), michael.l.tuite@jpl.nasa.gov (M.L. Tuite), david.flannery@qut.edu.au (D.T. Flannery), wmans@unm.edu (W.W. Mans), gpwilson@uw.edu (G.P. Wilson Mantilla).

https://doi.org/10.1016/j.palaeo.2021.110451
Received 9 August 2020; Received in revised form 25 April 2021; Accepted 3 May 2021
Available online 8 May 2021

composition, especially on short temporal scales (Grandpre et al., 2013; Therrien et al., 2007).

The end-Cretaceous mass extinction resulted in the extinction of non-avian dinosaurs, ammonites, and many other important terrestrial and marine taxa (e.g., Fastovsky and Bercovici, 2016; Henehan et al., 2019; Landman et al., 2014; Longrich et al., 2012). At the Cretaceous-Paleogene (K-Pg) boundary (KPB) an approximately 2‰ negative excursion in $\delta^{13}C$ is reported in both terrestrial organic carbon (Arens and Jahren, 2000; Arinobu et al., 1999; Bourque et al., 2021; Grandpre et al., 2013; Maruoka et al., 2007; Schimmelmann and DeNiro, 1984; Therrien et al., 2007) and marine inorganic carbon in many (but not all) sections (D'Hondt, 2005; Keller and Lindinger, 1989; Schulte et al., 2010; Sepúlveda et al., 2019). This excursion is interpreted to have been the result of a significant perturbation to the carbon cycle associated with the asteroid impact that substantially or entirely drove the K-Pg mass extinction (Archibald et al., 2010; Hull et al., 2020; Schulte et al., 2010).

Here we present results from sedimentary organic carbon isotope ($\delta^{13}C_{org}$) sampling across the KPB from the Hell Creek region of Garfield County in northeastern Montana, USA (Fig. 1). The Hell Creek region has featured prominently in debates regarding the timing and causes of the K-Pg mass extinction in the terrestrial realm (Archibald and Clemens, 1982; Clemens et al., 1981; Smit and Van Der Kaars, 1984; Wilson, 2014). In this region, the Hell Creek Formation (Khc; mostly Cretaceous) and Tullock Member of the Fort Union Formation (Pgft; mostly Paleogene) compose a record of nearly continuous alluvial, lacustrine, and palustrine deposition that spans the KPB, with the boundary clay itself often being recognized locally (within our sampling area, Fig. 1) as nearly synchronous with the lithological contact between the Khc and Pgft (Fig. 2) (Baadsgaard et al., 1988; Fastovsky and Bercovici, 2016; Hartman et al., 2014; Moore et al., 2014). As such, the Hell Creek region has a rich history of paleontological (Archibald, 1982; Horner et al., 2011; Lofgren, 1995; Scannella et al., 2014; Smith et al., 2018; Wilson, 2014; Wilson, 2013; Wilson, 2005) and geological research (Fastovsky, 1987; Fendley et al., 2019; Hartman et al., 2014; Ickert et al., 2015; Noorbergen et al., 2018; Sprain et al., 2018; Sprain et al., 2015; Tobin et al., 2014).

Previous $\delta^{13}C_{org}$ studies in this region (Arens et al., 2014; Arens and Jahren, 2002; Arens and Jahren, 2000; Gardner and Gilmour, 2002; Maruoka et al., 2007) have argued that a $\delta^{13}C_{org}$ excursion at or near the KPB is correlative with the globally recognized marine carbon isotope excursion, though the interpretation of these records as globally relevant has been questioned (Grandpre et al., 2013). The duration of the proposed KPB $\delta^{13}C$ excursion differs by several orders of magnitude depending on the location examined (Arens and Jahren, 2000; Sepúlveda et al., 2019), which makes it difficult to determine which records reflect global atmospheric effects, and which are driven by local conditions. In the Hell Creek region, the proposed $\delta^{13}C_{org}$ excursion likely

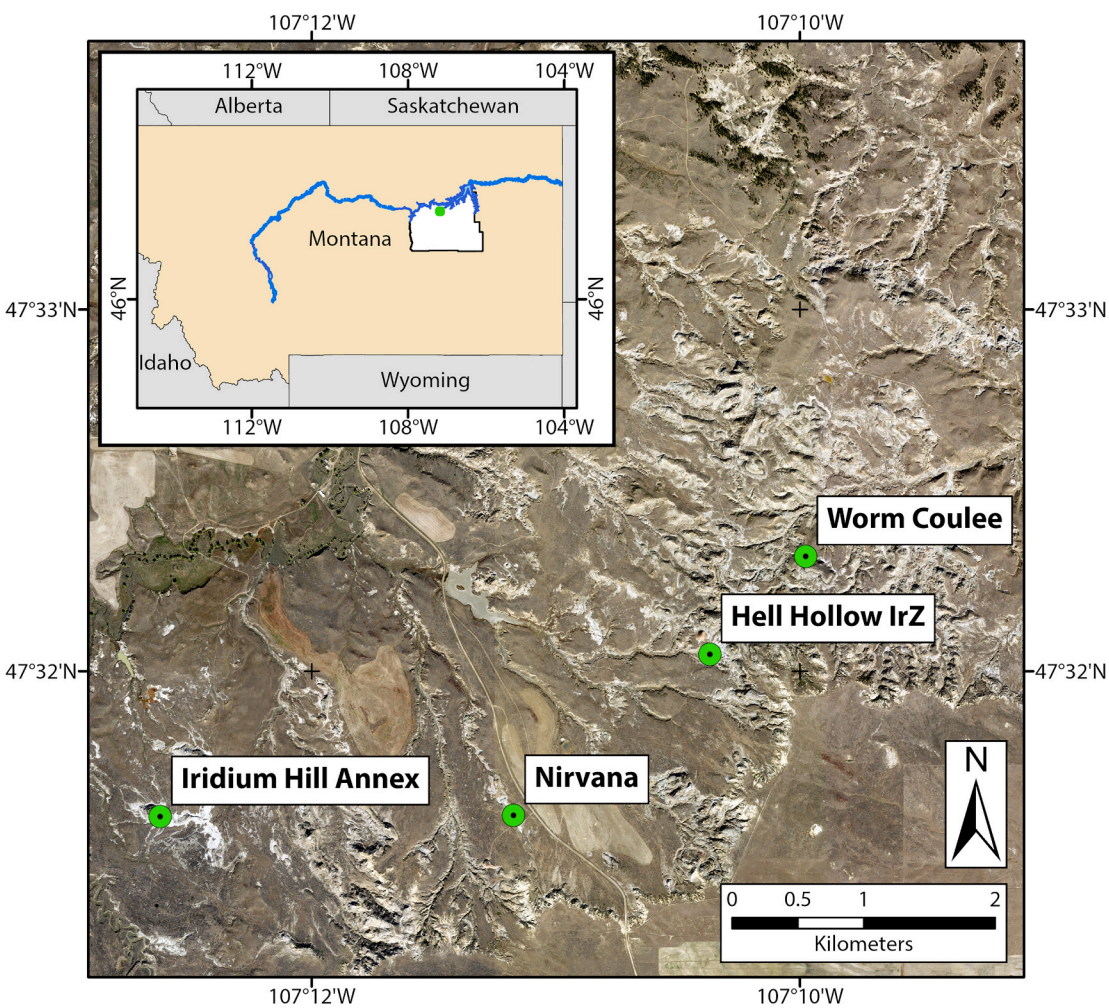

Fig. 1. Location of three sampling sites on satellite imagery (Google Earth Pro). Nirvana was sampled with hand trenches, backhoe-excavated trenches and cores, whereas Iridium Hill Annex and Worm Coulee were sampled with hand trenches (also see Fig. S9). Hell Hollow IrZ was recognized by Sprain et al. (2015) and can be laterally traced to Worm Coulee. Inset - location of sampling area (green dot) within Garfield County (white), Montana, USA, with Missouri River and Fort Peck Reservoir in blue. (For interpretation of the references to colour in this figure legend, the reader is referred to the web version of this article.)

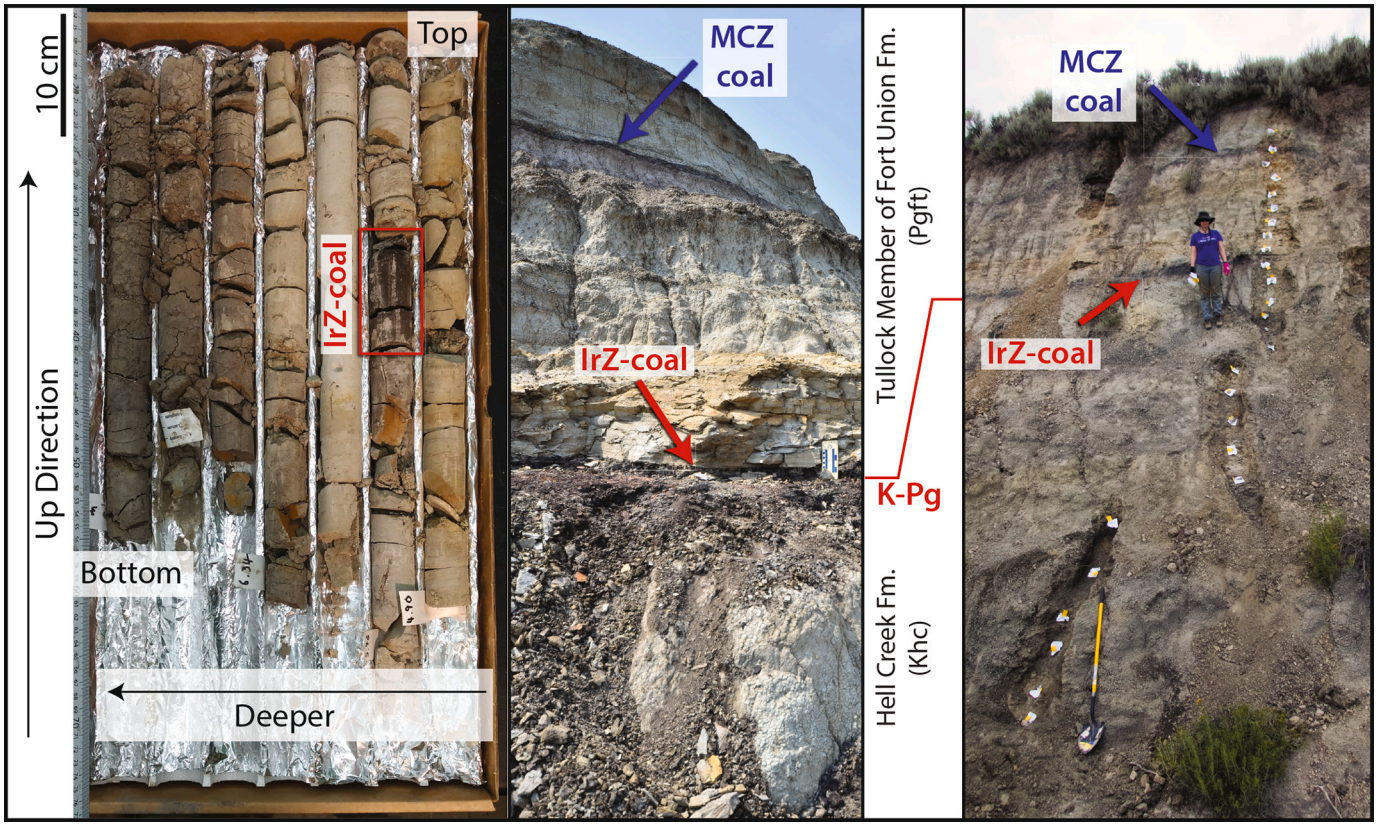

Fig. 2. Photos of core and outcrop sampling in their stratigraphic context. (Left) one box of core recovered from the upper drill hole (N1) at Nirvana. Note top is to the right, scale to the left of the image. (Middle) IrZ coal exposure at Nirvana (image facing to south), at the site of ash recovery used to assign age to Nirvana (Sprain et al., 2015). Note scale bar at right of image. (Right) Hand trench at Nirvana (image facing to east), shovel and human for scale. Sample bags indicate locations of rock sample collection. IrZ coal here can be traced laterally 30 m to outcrop in middle image (Fig. S9). MCZ is the McGuire Creek Z coal from which a distinct bentonite has been recognized (see Section 2.3).

lasted less than 10 k.y. before returning to pre-excursion values (Renne et al., 2013), but many marine records show carbon isotope recovery that lasted 100–1000 k.y. (e.g., D'Hondt, 2005). This difference in duration between continental and marine records has been used to argue that the terrestrial biosphere recovered more quickly from the extinction (Arens and Jahren, 2000), and these short duration excursions have guided modeling of this time period (e.g., Milligan et al., 2019). However, substantial decoupling between the duration of marine versus terrestrial carbon isotope excursions has not been noted in other global carbon cycle disruptions; for example, continental and marine carbon isotope records from the Paleocene-Eocene Thermal Maximum have similar durations, on the order of 100 k.y. (Tipple et al., 2011).

1.2. Motivation

This study tests the importance of two factors that may complicate bulk sedimentary $\delta^{13}C_{org}$ records, particularly those taken from continental paleoenvironments. Specifically, we test the effects of (1) modern surficial weathering and/or contamination, and (2) changing depositional environments, as reflected by differences in lithology. We then test whether these factors complicate interpretation of $\delta^{13}C_{org}$ records across the KPB. There are other factors that may affect $\delta^{13}C_{org}$ values, including burial diagenesis, but our tests focus on sections that are within 3 km of each other and have experienced an identical burial history.

First, modern surface conditions may affect sedimentary organic carbon records obtained from bulk sediment. Depositional organic carbon may be altered or removed through a variety of processes, including oxidation, dissolution, or bacterial metabolism (See supplementary material for quantitative discussion of these processes). These processes have the potential to fractionate carbon, altering the $\delta^{13}C_{org}$ value of the remaining organic material. Additionally, modern plants may contribute carbon to the sedimentary organic pool through root infiltration, which if unrecognized will bias the $\delta^{13}C_{org}$ value of sedimentary organic material. This effect can be strong because modern C4 plants (approximately −13‰ VPDB) have much higher $\delta^{13}C_{org}$ values (e.g., Morgan et al., 1994) than Cretaceous plants, which exclusively used the C3 photosynthetic pathway (approximately −27‰ VPDB).

Second, bulk sediment from different continental depositional environments may record different $\delta^{13}C_{org}$ values due to the deposition of different plant species, or even different tissues from the same plant (e.g., leaves vs. woody debris), which can have measurably different isotopic values (e.g., Bögelein et al., 2019; Graham et al., 2019). River migration or avulsion can rapidly change the local environment from fluvial to palustrine or lacustrine (e.g., Hupp et al., 2019). If these different environments accumulate carbon with different $\delta^{13}C_{org}$ values, these geologically rapid facies shifts may be accompanied by equally rapid $\delta^{13}C_{org}$ changes without any shift in the $\delta^{13}C$ value of atmospheric CO_2. The spatial heterogeneity of continental environments can potentially affect not only the stratigraphic (and therefore temporal) record of $\delta^{13}C_{org}$, but also the spatial record, meaning temporally correlative sections could record different $\delta^{13}C_{org}$ patterns (see Beerling and Royer, 2002 for further discussion of these issues).

1.3. Testing

Previous work in the Hell Creek region (Arens et al., 2014; Arens and Jahren, 2002; Arens and Jahren, 2000) argues for two hypotheses that

we test here: (1) original $\delta^{13}C_{org}$ values recovered from hand trenches are not altered due to surface weathering or contamination, and (2) the $\delta^{13}C_{org}$ of terrestrial organic matter is regionally consistent, regardless of local-scale depositional (and therefore lithological) variation. Those authors concluded that both hypotheses were supported, and subsequently that negative $\delta^{13}C_{org}$ excursions can be used as chemostratigraphic markers, most notably to recognize the KPB (see Section 5.2).

To test whether modern surficial processes can alter sedimentary $\delta^{13}C_{org}$ values, we employed three different sampling methods at nearly the same location to test whether surface diagenetic effects create measurable differences in the $\delta^{13}C_{org}$ values (see Section 5.1). Specifically, sediment samples were obtained from shallow trenches dug by hand, a deep trench dug by an excavator, and sediment cores.

We also tested the effects of depositional control on $\delta^{13}C_{org}$ values by applying the same hand-trenched sampling method to three sites across a ~ 3 km^2 area and controlling for lithology in our data analysis. We then compared our results with previously published data to test whether terrestrial $\delta^{13}C_{org}$ records can be used to unambiguously identify the KPB and constrain atmospheric conditions in the immediate aftermath of the Chicxulub bolide impact (see Sections 5.2.1, 5.2.2).

2. Geologic setting

2.1. Geologic overview

The Khc is largely composed of meter-bedded, drab-colored mudstone and sandstone, typically with gradational contacts between beds. In contrast, the Pgft is largely composed of dm- to m-bedded, more brightly-colored mudstone and sandstone beds with sharp, clearly defined contacts between beds. Bedding contacts are particularly evident at laterally continuous lignite and coal layers; the maturity of these lithologies varies, but hereafter we will use "coal" to indicate these lithologies (see Hartman et al., 2014 for a detailed discussion of the lithological and temporal relationships). The base of the Pgft is defined as the lowest stratigraphic occurrence of a locally laterally continuous coal or lignite (the Z coal; Collier and Knechtel, 1939), though the definition of the Z coal based on thickness has resulted in some conflicted definitions, and the identification of multiple Z coals within a Z coal complex (see Moore et al., 2014 for further discussion). Additionally an older "null coal" within the Khc has been recognized east of our field area that does not fit this description of the contact (Lofgren, 1995; Sprain et al., 2015).

Even focused on the lowest Z coal, it is clear that the Z coal is not perfectly isochronous across the Hell Creek region (Fastovsky and Dott, 1986; Sprain et al., 2015). However, in many cases, including those at and near our sample sites, the basal Paleogene iridium anomaly is found within a claystone comprised of impact debris ("impact claystone") at the base of, or within, the Z coal (Moore et al., 2014). In these cases, the Z coal is more specifically termed the Iridium Z coal, or IrZ coal, making this bed a marker for the KPB. For clarity, and to distinguish between multiple named Z coals in the region (e.g., McGuire Creek Z, Hauso Flats Z) we follow previous convention (Ickert et al., 2015; Sprain et al., 2015; Swisher III et al., 1993), and use the term IrZ coal for any coal that is correlated with a coal containing the iridium anomaly using geochronology, geochemistry, or lateral tracing.

With the exceptions of some sandstone and siltstone strata, both the Khc and Pgft are not strongly lithified, and are relatively easy to excavate with hand tools. We have noted from previous excavations in this area that the modern root invasion is pervasive and quite deep (>1 m) in many locations, and that precipitation and temperature exhibit significant seasonal variation in the region. Common modern plants include sagebrush (C3), grasses (C4), saltbushes (C4), as well as a variety of other flora (Brown, 1971), with rooting depths in similar climates exceeding one meter (Schenk and Jackson, 2002). Consequently, it can sometimes be difficult to access definitively unaltered material with hand tools.

2.2. Sampling

To test the effects of modern surficial contamination and/or weathering, we used three different methods to obtain samples from a small hill named Nirvana (Figs. 1, 2, Fig. S9) (Arens and Jahren, 2002; Fendley et al., 2019; Ickert et al., 2015; Sprain et al., 2015). This site is less than 1 km from several other sites where an iridium anomaly has been identified from within the IrZ coal, including Herpijunk Promontory and Iridium Hill (Alvarez, 1983; Arens and Jahren, 2000; Smit and Van Der Kaars, 1984; Swisher III et al., 1993). Nirvana is a roughly oval shaped hill, approximately 60 m long by 30 m wide, and about 10 m tall at the largest exposure (Fig. 2, Fig. S9). The top is subhorizontal, and the sides are steep, with relatively good exposure of sedimentary strata visible from most angles (Figs. 1, 2).

Three different sampling techniques were used at Nirvana: (1) hand trench, (2) backhoe trench, and (3) a drilled core (Fig. 2, Fig. S9). A set of samples was obtained from a trench dug to approximately 0.5 m below the surface with hand tools. The trench depth varied somewhat with slope, with the goal of obtaining visually less altered and more competent rock at depth. Samples were taken every 30 cm across 7.5 m of exposed section. A second set of samples was obtained from a trench excavated with a backhoe to approximately 1 m below the surface, a depth that was limited by access to the outcrop and the capabilities of the backhoe. This section was sampled every 10 cm. A third set of samples were obtained from two sediment cores drilled near the center of the hill, one sampling the upper part of the section (N1), and the other sampling the lower (N2). In total, 13.6 m of stratigraphy was cored, though some overlap between the cores results in a shorter total stratigraphic coverage. Cores were sampled at ~10 cm intervals.

To test how lithology and spatial variability affect the $\delta^{13}C_{org}$ record over the same stratigraphic interval, two additional locations were sampled with hand trenching (Fig. 1). The first, named Iridium Hill Annex (Fendley et al., 2019), is a larger hill immediately adjacent to Iridium Hill (Fig. S9), one of the first terrestrial sites in the world at which the K-Pg iridium anomaly was recorded (Alvarez, 1983; Smit and Van Der Kaars, 1984). This anomaly is recorded within a thin claystone layer immediately below the IrZ coal. This site is well exposed, including the uppermost few meters of the Khc and a much thicker record of Pgft than the other sites sampled in this study. The second site, Worm Coulee (Fig. 1, Fig. S9), is located near the Worm Coulee 1 vertebrate microfossil bonebed, one of the most well-sampled early Paleocene fossil localities in North America (Archibald, 1982; Wilson, 2014). The Worm Coulee 1 locality is hosted in a poorly consolidated sandstone that is interpreted as a Paleocene-age channel deposit that eroded below the Z coal locally (Archibald, 1982). Our Worm Coulee samples were collected from a hand-trenched section ~60 m south of Worm Coulee 1 where a thin remnant of the IrZ coal remains exposed, along with ~10 m of the uppermost Khc below and ~ 15 m of the lowermost Pgft above. Our sampling was limited to ~2 m above the IrZ coal due to extensive vegetative cover of the upper Pgft beds in that location. Both sections were sampled at 30 cm intervals.

2.3. Correlation and age control

All three sites can be correlated based on the presence of locally defined IrZ coal identifiable in outcrop. At Nirvana, the IrZ coal marking the Khc-Pgft contact is visible in outcrop and cores (Figs. 2, 3A, D), and laterally traceable between all sampling methods at this site. Though not being measured for iridium directly, the Z coal at Nirvana has previously been correlated to known IrZ coals through geochronological and geochemical (Pb isotope) analysis of the Nirvana bentonite layer within the coal bed, which crops out roughly ~2 cm above the measured Ir-anomaly (within the impact claystone) at the Iridium Hill locality (Ickert et al., 2015; Sprain et al., 2015). Additionally, the McGuire Creek bentonite has been geochemically identified at the Nirvana locality within a thin organic rich siltstone ~2.5 m above the IrZ coal (Ickert

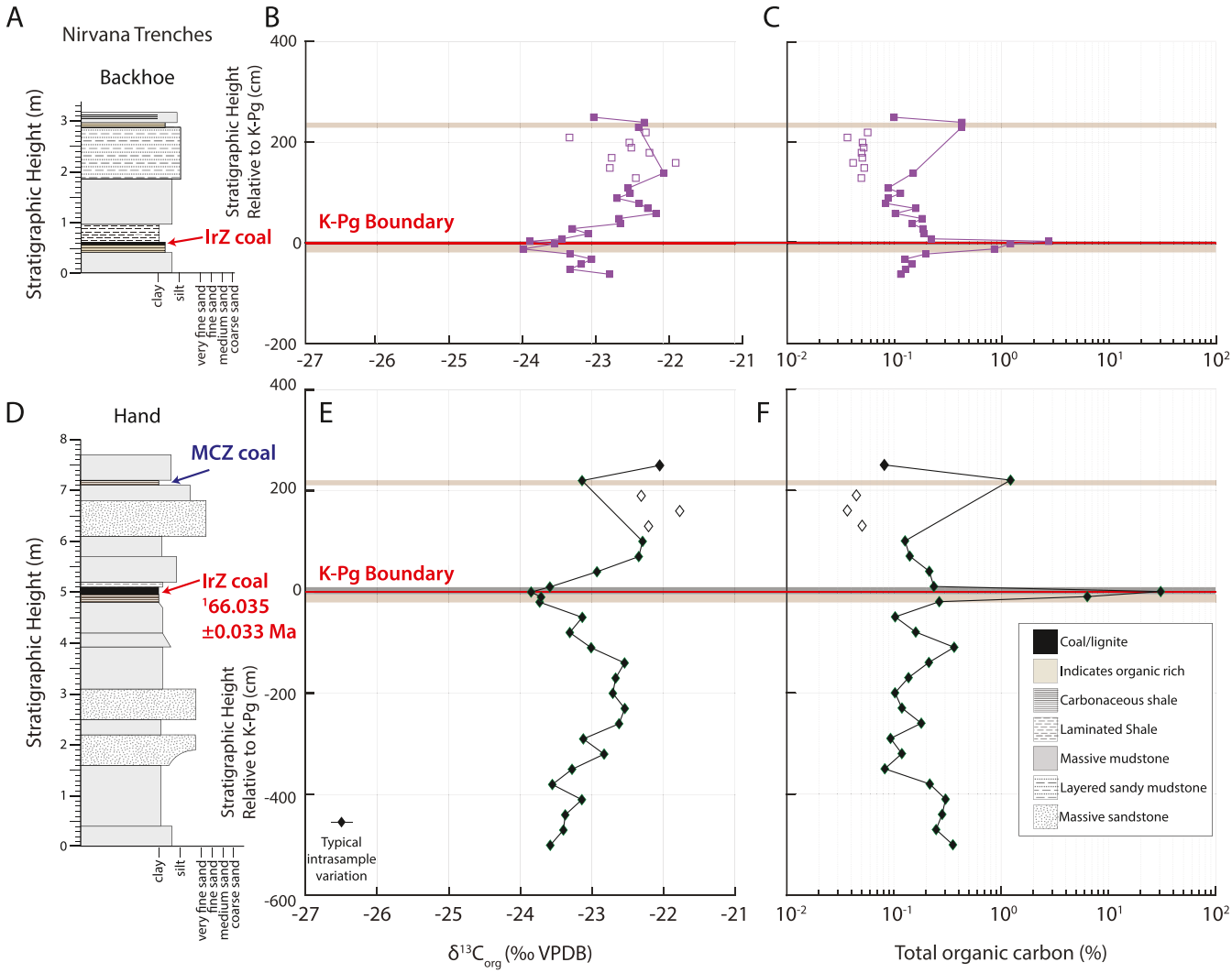

Fig. 3. Sedimentological log (A, D), organic carbon isotope record (B, E), and total organic carbon (C, F) for two trenched sections at Nirvana. At top, the trench dug with a backhoe, and at bottom the trench dug by hand. Solid symbols represent samples for which reliable amounts of organic carbon were obtained for isotopic analysis. Open symbols represent samples from which only low amounts of organic carbon could be obtained, and thus $\delta^{13}C_{org}$ values should be considered unreliable. Typical instrumental uncertainty is within data point size, while typical intra-sample variation on $\delta^{13}C_{org}$ replicates (0.35‰) shown at bottom left of (E). Black and brown bands in (B, C, E, F) highlight intervals of coal and carbonaceous shale, respectively. [1]Age assignment based on ash (Nirvana bentonite) within IrZ coal at this location from Sprain et al. (2015) (see Section 2.3). Note, the age also applies to the IrZ coal identified in A. (For interpretation of the references to colour in this figure legend, the reader is referred to the web version of this article.)

et al., 2015). The McGuire Creek bentonite has been found in several KPB sections in McCone County (adjacent to the east of Garfield County) and has been dated to be within the first 25 k.y. of the Paleogene (Sprain et al., 2018). At Nirvana, sections were correlated in the field through direct lateral tracing of the IrZ coal between outcrop sections, and surveying with a hand level was used to place the core hole tops in relation to outcrop sections. This survey approach was consistent (within 10 cm) with lithological correlation of the outcrop sections to the cores using marker beds.

At Iridium Hill Annex the Khc-Pgft contact is identified by an IrZ coal, which contains the Nirvana bentonite (Ickert et al., 2015) (Fig. 4A), and is laterally traceable (~100 m) directly to the site of one of the first continental iridium anomaly records (Alvarez, 1983). Several other lignites and coals are recognized in the overlying Pgft section (Fig. 4), including the Hauso Flats Z coal, dated to 65.990 ± 0.020 (1σ) Ma (Renne et al., 2013; Swisher III et al., 1993). At both Nirvana and Iridium Hill Annex, the Khc-Pgft contact is therefore within 10 cm of the KPB.

The Khc-Pgft contact at Worm Coulee is also identified by a lowest thin (3–5 cm) lignite layer (Z coal), but the placement of the KPB with respect to this coal is less well-defined due to a need to trace beds further to a nearby measured location. The Z coal at Worm Coulee can be laterally traced to a site ("Hell Hollow") that is approximately 700 m away (Fig. 1), where Sprain et al. (2015) dated an ash from within the Z Coal (700 m) to 66.061 ± 0.039 (1σ) Ma, which is within analytical precision of dates (66.043 ± 0.011 (1σ) Ma) generated from within the IrZ coal elsewhere (Renne et al., 2013) (Fig. 5). This same ash bed was also identified geochemically as the Nirvana bentonite (Ickert et al., 2015), which as previously mentioned, is within a few cm of the impact claystone at Iridium Hill. There is no evidence for either the bentonite or impact claystone at Worm Coulee, but we cannot determine (i) if they were eroded during deposition of the overlying sandstone, (ii) if those layers were never deposited at this location, or (iii) if they were deposited, but not within the Z coal. Given the continuous lateral trace of the Z coal at Worm Coulee to the IrZ coal to Hell Hollow, the first explanation (i) is more likely, and we will refer to the lowest coal at Worm Coulee as the IrZ coal hereafter.

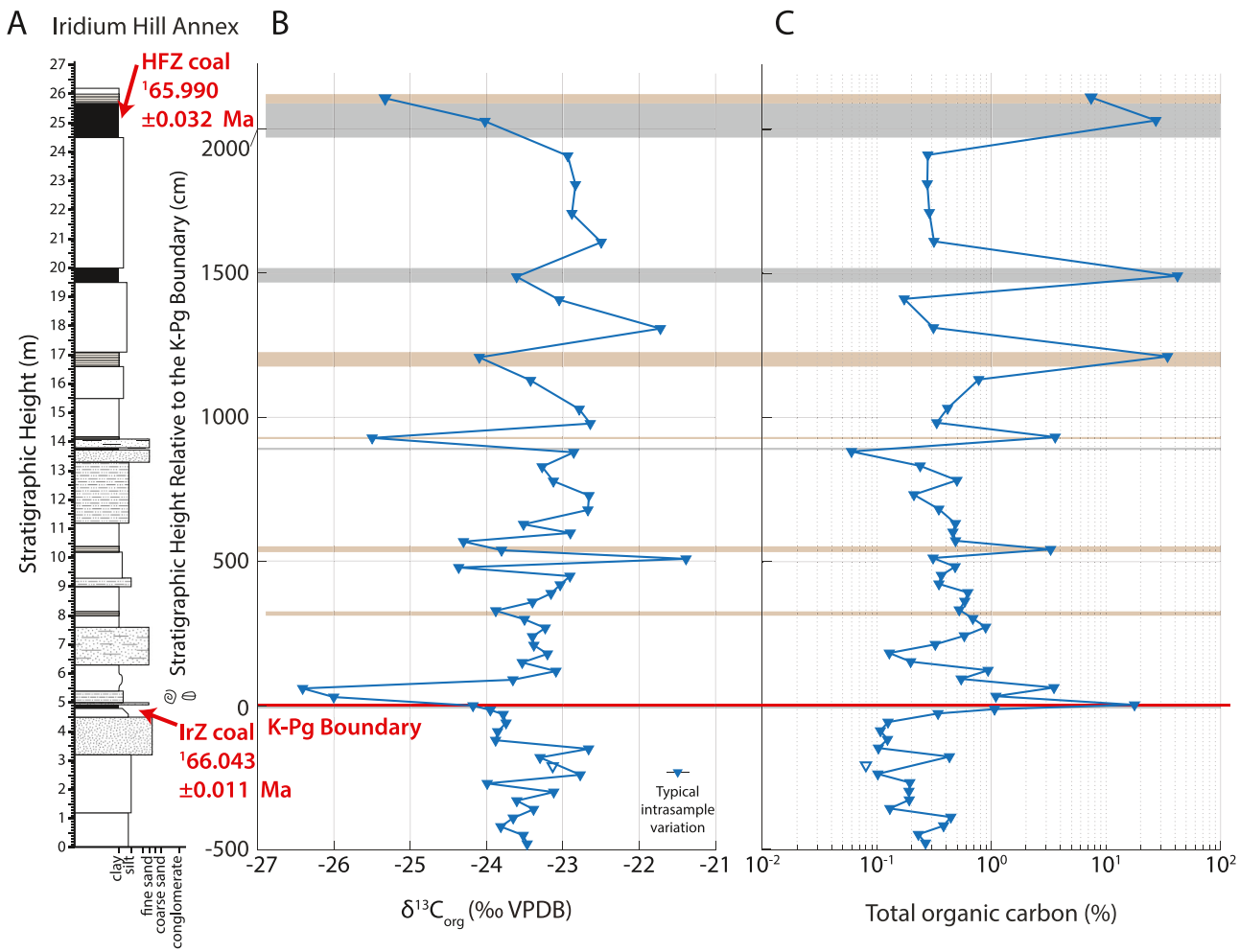

Fig. 4. Sedimentological log (A), organic carbon isotope record (B), and total organic carbon (C) for hand-trenched section at Iridium Hill Annex. Solid symbols represent samples for which reliable amounts of organic carbon were obtained for isotopic analysis. Open symbols represent samples from which only low amounts of organic carbon could be obtained, and $\delta^{13}C_{org}$ values should be considered unreliable. Typical instrumental uncertainty is within data point size, whereas typical intra-sample variation on $\delta^{13}C_{org}$ replicates (0.35‰) shown at bottom right of (B). Black and brown bands in (B, C) highlight intervals of coal and carbonaceous shale, respectively. [1]Age assignment based on ash within IrZ coal at this location from Renne et al. (2013) (see Section 2.3). (For interpretation of the references to colour in this figure legend, the reader is referred to the web version of this article.)

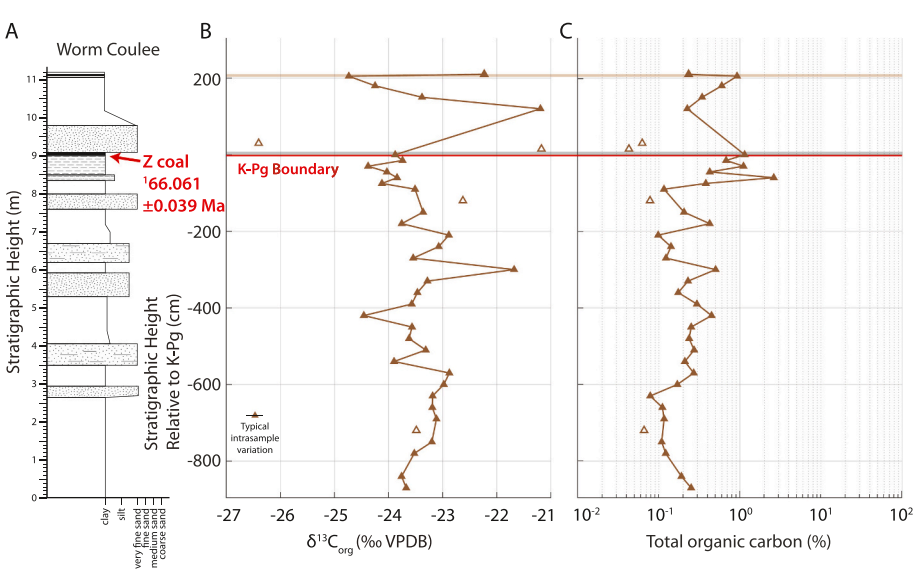

Fig. 5. Sedimentological log (A), organic carbon isotope record (B), and total organic carbon (C) for hand-trenched section at Worm Coulee. Solid symbols represent samples for which reliable amounts of organic carbon were obtained for isotopic analysis. Open symbols represent samples from which only low amounts of organic carbon could be obtained, and $\delta^{13}C_{org}$ values should be considered unreliable. Typical instrumental uncertainty is within data point size, whereas typical intra-sample variation on $\delta^{13}C_{org}$ replicates (0.35‰) shown at bottom right of (B). Black and brown bands in (B, C) highlight intervals of coal and carbonaceous shale, respectively. [1]Age assignment based on ash within IrZ coal from nearby (< 700 m) Hell Hollow locality from Sprain et al. (2015). (For interpretation of the references to colour in this figure legend, the reader is referred to the web version of this article.)

3. Methods

3.1. Field sampling

Hand trenches at Nirvana, Iridium Hill Annex and Worm Coulee were dug with rock hammers and picks, and the deeper trench was excavated with a backhoe at Nirvana. Rock samples were obtained from trenches in the field using standard field tools (e.g., hammers, trowels) and placed in aluminum foil to avoid organic contamination from sample bags. Samples were placed in their stratigraphic context as the section was measured (Jacob's staff and Abney level) and logged, typically at dm resolution. Two cores were drilled at Nirvana using a Shaw Backpack drill lubricated with water. The first core (N1) was spudded on the top of the Nirvana hill (Fig. S9) and terminated at just over 7 m depth when drilling progress slowed significantly. The upper 20–30 cm of loose material and soil on the surface was removed prior to drilling. Coring rates through rocks with significant clay content were slowed, likely due to fouling of the diamond abrasive bit, but progress in mudstones was improved by adding notches to a continuous diamond-coring bit. Coring was much faster in sandstones, and overall coring rates were about 3 m of recovery per day. This coring equipment is compact but requires removal of the entire drill string in order to recover core and to add length, and therefore the drilling rate decreases quickly with depth. Consequently, a second core was started on a lower, completely barren, flat area on northern end of the Nirvana hill 50 m to the northeast (Fig. S9), starting ~1 m stratigraphically above where the first core finished to ensure overlap between the two cores (Fig. 6A). This second core (N2) proceeded to a depth of 7 m, though the topmost ~50 cm was unrecoverable. To avoid contamination during sampling of the core material in the lab, the core surface was abraded at the sampling location, and samples were often taken from the interior of the core when pre-existing breaks were located appropriately.

The composite of these two cores captured ~13 m of rock spanning the Khc-Pgft contact. Core recovery was greater than 90%, and possibly as a high as 100% accounting for minor compaction of clay layers (except for the uppermost ~0.5 m of N2). The cored material was typically better consolidated than samples from trenches, but was still friable, easily fracturing into short lengths (Fig. 2). Logging and sampling of cores was completed in a laboratory setting using standard tools, typically at cm resolution.

3.2. Lab methods

Portions of the rock samples were separated for organic carbon analysis, whereas the remainder was preserved as an archive. Samples were crushed with an agate mortar and pestle if possible, or with a ceramic puck mill in Spex Shatterbox for harder samples. Although no modern plant material was observed in situ during field sampling, occasional fine rootlets were detected during sample disaggregation; any found were discarded along with surrounding material. Crushed samples were acidified using standard techniques previously employed successfully with these sediments (Arens et al., 2014). Briefly, crushed material was weighed, placed in test tubes, and then acidified with 1.2 M HCl overnight. Tubes were then centrifuged, and the supernatant poured off, and if further acid reaction was observed, this step was repeated. After acidification, samples were rinsed three times, each time 18 MΩ H_2O was added, the sample was centrifuged, and then the supernatant poured off. Samples were then dried in the test tube at 60 °C for 1–3 days until dry. Acidified samples were homogenized, weighed, and placed in tin capsules before being introduced to a Costech elemental analyzer connected via continuous flow to Thermo Delta V+ housed at the Alabama Stable Isotope Laboratory. A run of ~30 samples were interspersed with ~5 low percent organic carbon standards (B2153: −26.66‰ vs. VPDB; TOC = 1.61%; from Elemental Microanalysis, Certificate 304,695). Standard deviation of sample $\delta^{13}C_{org}$ measurements, calculated from variation of isotopic standards, were < 0.1‰ for

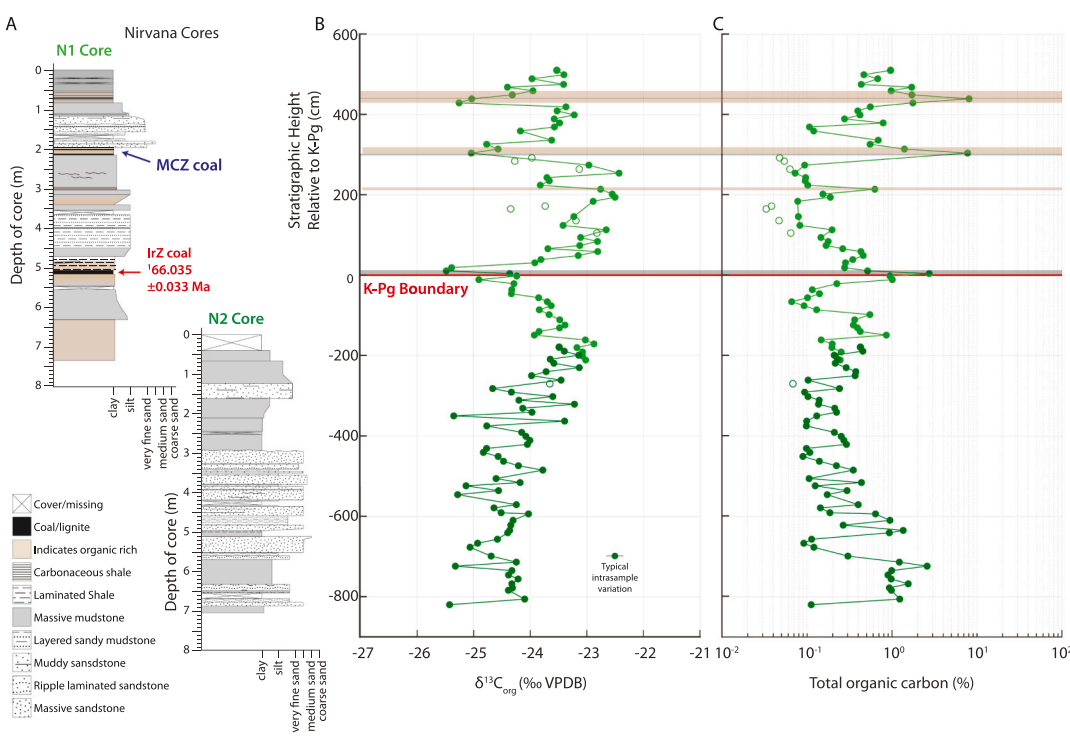

Fig. 6. Sedimentological logs (A), organic carbon isotope record (B), and total organic carbon (C) for two cores drilled at Nirvana. Solid symbols represent samples for which reliable amounts of organic carbon were obtained for isotopic analysis. Open symbols represent samples from which only low amounts of organic carbon could be obtained, and $\delta^{13}C_{org}$ values should be considered unreliable. Typical instrumental uncertainty is within data point size, whereas typical intra-sample variation on $\delta^{13}C_{org}$ replicates (0.35‰) shown at bottom right of (B). Black and brown bands in (B, C) highlight intervals of coal and carbonaceous shale, respectively. (For interpretation of the references to colour in this figure legend, the reader is referred to the web version of this article.)

each run. This approach limited sample size to roughly 45 mg of processed sediment powder, which in turn placed an effective lower limit of detectable organic carbon at about 0.03 wt% (see supplementary material). For replicate samples with adequate carbon ($n = 17$), the average $\delta^{13}C_{org}$ difference between replicates was 0.35‰, which is displayed in Figs. 3–6 to provide a guide to intra-sample variation.

3.3. Statistical methods

To visualize the difference in $\delta^{13}C_{org}$ values (Fig. 7A) derived from different sampling methods at Nirvana, we constructed LOWESS fits (span = 0.3) with 95% prediction intervals for each sampling method (Fig. 7B). To generate our fits and prediction interval bounds we used the methodology and LOWESS MATLAB script (mylowess.m, which calls smooth.m) of Shure (2011). To quantitatively compare the outcrops with cores, we assumed that the combined core data most closely captured the "true" record for the Nirvana site, and then determined the offset in $\delta^{13}C_{org}$ between the trenches and cores. To do so, we calculated the difference between the trenched $\delta^{13}C_{org}$ data and the value of the core LOWESS curve for the same stratigraphic height (see Section 4.2). The distribution of these offset values is shown in Fig. 8.

To assess whether $\delta^{13}C_{org}$ values were controlled by the environment of deposition, we categorized samples from all sections into simple lithological groups after Arens et al. (2014) (though we use the term "claystone" in place of "mudstone"). This categorization oversimplifies lithological complexity but allows statistical comparison of groups (Fig. 9A, Table 1). We then performed a Kruskal-Wallis test using the statistics toolbox in Matlab (The Mathworks, Inc., 2020) to determine whether lithology was a significant predictor of $\delta^{13}C_{org}$ (Section 4.3). Dunn-Šidák post hoc pairwise tests were then performed to see which lithologies had statistically significant differences in $\delta^{13}C_{org}$ from others; this test accounts for the fact that multiple comparisons were performed when assessing significance. We repeated this testing approach while separating organic rich lithologies immediately under or overlying the KPB from non-KPB organic rich lithologies to determine whether statistical differences in lithology were driven by different $\delta^{13}C_{org}$ values from the KPB associated samples in each section (see Section 5.2).

4. Results

4.1. Section data

4.1.1. Nirvana hand trench

A total of 28 samples were obtained from 7.7 m of exposed stratigraphic section, at a sampling interval of 30 cm, with an increase to 10 cm near the IrZ coal (Fig. 3D). Most samples ($n = 25$) had sufficient organic carbon to measure reliable $\delta^{13}C_{org}$ values, but a small number ($n = 3$) were too low to obtain reliable values given the maximum permitted sample size (see Section 3.2). The low organic samples were usually from sandstones or other sandier lithologies, a pattern previously observed in this area (Arens et al., 2014; Arens and Jahren, 2000). The $\delta^{13}C_{org}$ record from this section shows a negative excursion of ~1.4‰ spanning the Khc-Pgft contact (Fig. 3E). A trend towards more negative values begins 1.4 m below the contact, reaches a minimum within the IrZ coal, then returns to Khc values within the first meter of the Pgft. This negative excursion is superimposed on an overall positive

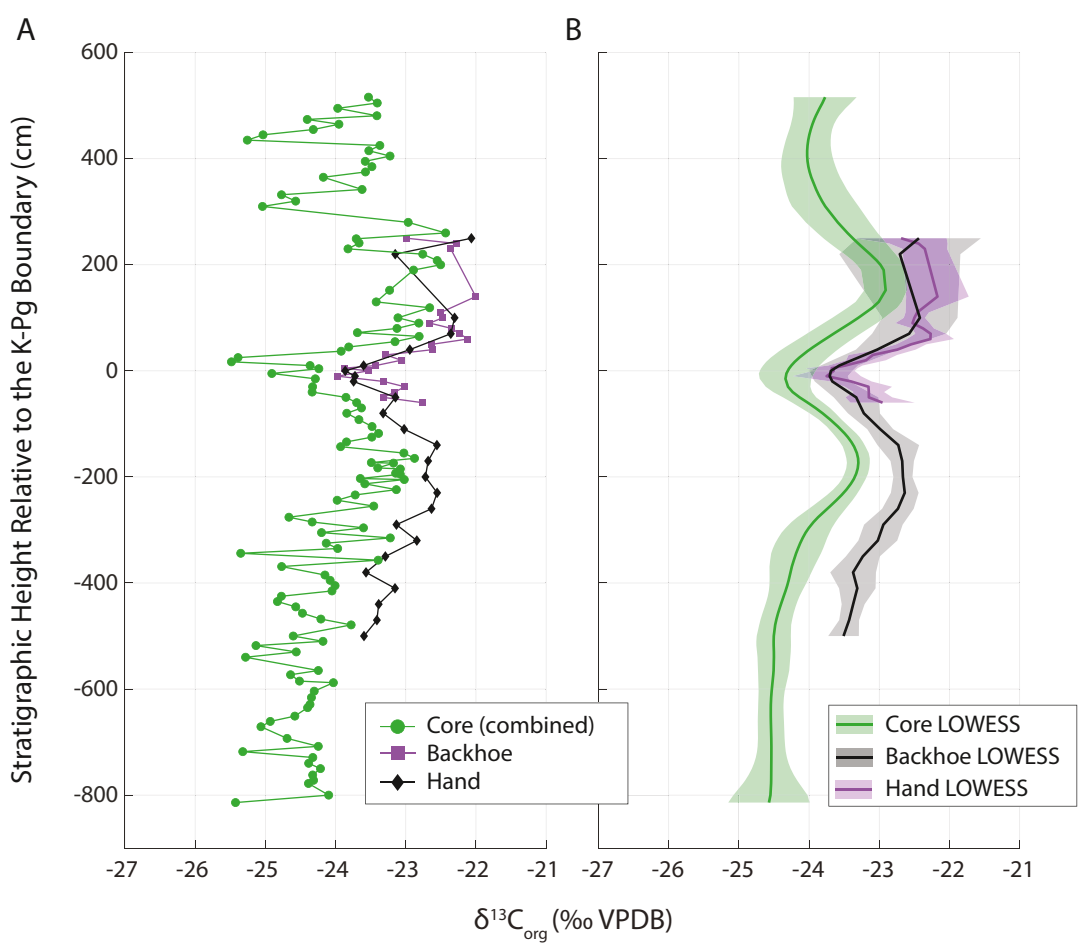

Fig. 7. (A) Stratigraphic comparison of $\delta^{13}C_{org}$ records from different sampling methods at Nirvana. The two core records are combined here, shown separated in Fig. 6. (B) LOWESS curve fits for each data set in (A) with 95% prediction interval shown with shaded regions.

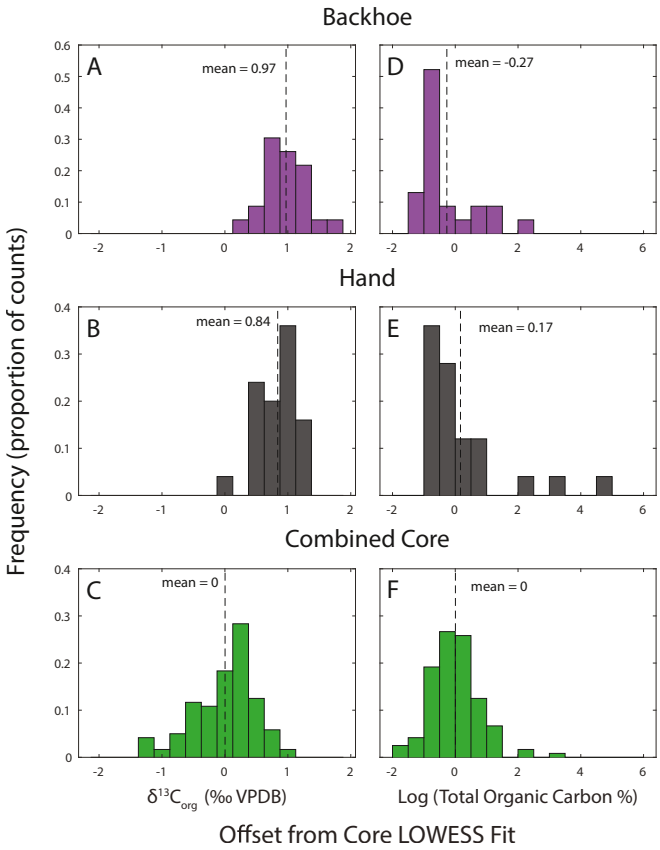

Fig. 8. Calculated offsets between $\delta^{13}C_{org}$ (A-C) and total organic carbon (D—F) for samples from each Nirvana section and the LOWESS fit from the combined core record (Fig. 7B) for the same stratigraphic height (see text). Vertical dashed lines indicate mean offset values.

trend of 1.5‰ from the bottom of the measured section to the top, though interpretation of the uppermost part of the section is complicated by low organic carbon content in sandy layers in the Pgft.

4.1.2. Nirvana backhoe

A total of 33 samples from 3.1 m of section exposed by the backhoe were sampled at a typical sampling interval of 10 cm (Fig. 3A). A larger proportion of these samples (10 of 33) were below ideal organic carbon concentrations given maximum sediment sample sizes (Fig. 3C). These samples were mostly from a sandy siltstone bed near the uppermost part of the section (Fig. 3A, C). As in the hand trench, this section shows a negative $\delta^{13}C_{org}$ excursion of at least 1.1‰ associated with the Khc-Pgft contact (Fig. 3B). Although this excursion also begins below the contact, the stratigraphically short section exposed in the Khc precludes a definitive determination of the onset of this part of the excursion. Organic carbon isotope values return to pre-excursion levels quickly within the Pgft, arguably within 0.5 m, though, as in the hand-trenched samples, there is an overall trend towards more positive $\delta^{13}C_{org}$ values upsection.

4.1.3. Nirvana cores

Samples were obtained from two cores, each a little over 7 m in length, with a recovered stratigraphic overlap of approximately 0.5 m (Fig. 6A). Cores were sampled at approximately 10 cm intervals, resulting in a total of 131 samples, almost all ($n = 123$) of which had sufficient organic carbon for reliable measurement. As in the other Nirvana sections, most of the low organic carbon samples come from sandier beds within the Pgft (Fig. 6C). A negative excursion of greater than 2.0‰ begins about 1.75 m below the Khc-Pgft contact and returns to background levels within 1.0 m of the Pgft. An overall positive trend of about 2.0‰ in $\delta^{13}C_{org}$ persists from approximately 5.0 m below the Khc-Pgft contact to about 2.0 m above the contact (Fig. 6B). In the uppermost 4.0 m of the section, three short, negative $\delta^{13}C_{org}$ excursions correspond with organic rich lithologies (Fig. 6B).

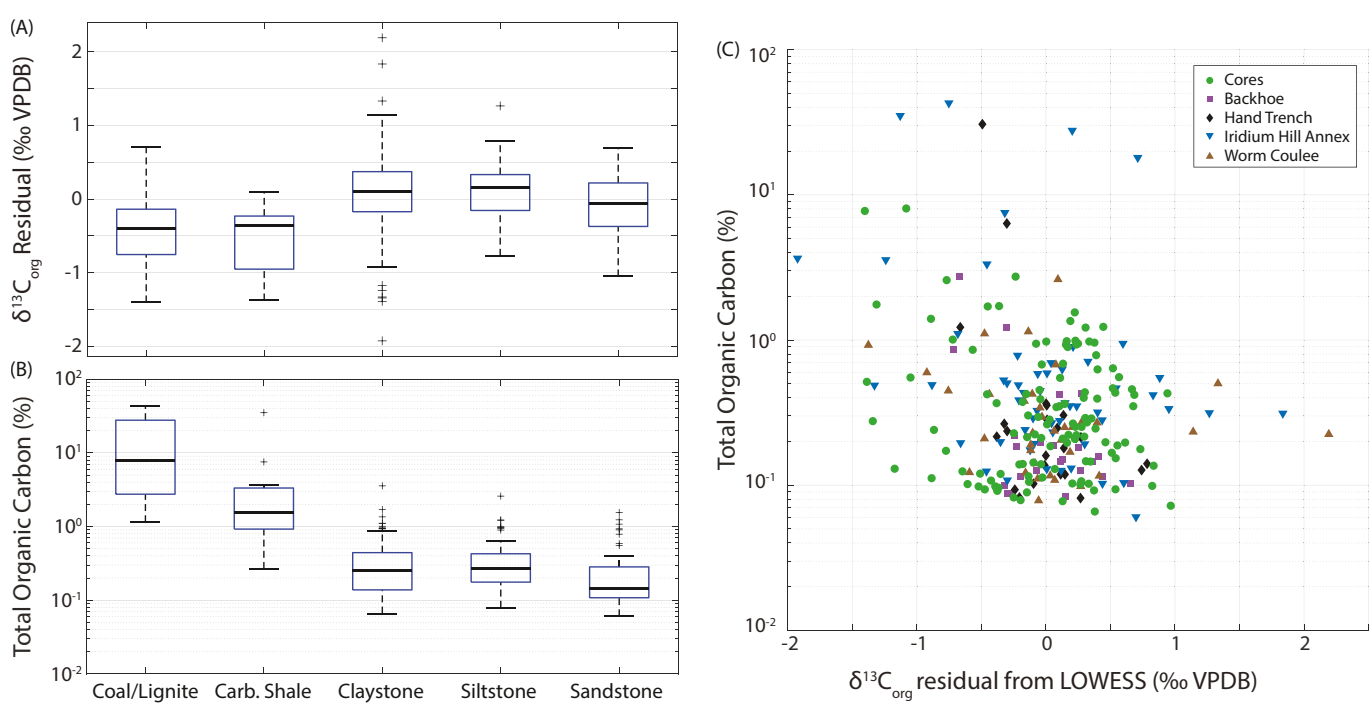

Fig. 9. (A) Boxplot of $\delta^{13}C_{org}$ values and (B) total organic carbon values for five different lithological categories, showing median (red line), 25th and 75th percentiles (blue box), and outliers (black cross). See also Table 1. (C) Covariance between $\delta^{13}C_{org}$ residuals and total organic carbon for all sampled sections. (For interpretation of the references to colour in this figure legend, the reader is referred to the web version of this article.)

Table 1
Comparison of $\delta^{13}C$ residuals from LOWESS fits, and total organic carbon values based on lithology.

Lithology	n	Mean $\delta^{13}C_{org}$ res. (‰ VPDB)	Std. dev. (‰ VPDB)	Pairwise Comparison *p*-values			
Coal/Lignite	10	−24.2	0.51	*Coal/Lignite*	*Carb. Shale*	*Claystone*	*Siltstone*
Carb Shale	13	−24.1	0.77	1.000	–	–	–
Claystone	137	−23.4	0.82	0.016*	0.017*	–	–
Siltstone	48	−23.4	0.70	0.018*	0.021*	0.999	–
Sandstone	51	−24.0	0.73	0.962	0.996	.001*	0.004*

Lithology	n	Mean TOC (%)	Std. dev. (%)	Pairwise Comparison *p*-values			
Coal/Lignite	10	14.81	14.38	*Coal/Lignite*	*Carb. Shale*	*Claystone*	*Siltstone*
Carb Shale	13	4.47	9.39	0.995	–	–	–
Claystone	137	0.39	0.48	2.88E-06*	4.06E-05*	–	–
Siltstone	48	0.42	0.44	5.31E-05*	7.40E-04*	1.000	–
Sandstone	51	0.29	0.31	9.1E-09*	1.11E-07*	0.074	0.075

Pairwise comparison *p*-values generated from a Dunn-Šidák post hoc test (see text); *indicates comparisons <0.05.

4.1.4. Iridium Hill Annex

Samples were obtained from 26.1 m of hand-trenched sections, with most of the sampled interval in the Pgft (Fig. 4, Fig. S9). A total of 57 samples were obtained at a sampling resolution of 30 cm in the lower half of the section, with lower resolution (0.5–1.0 m) sampling in the upper half of the section. All but two samples had sufficient organic carbon for reliable $\delta^{13}C_{org}$ measurements. At Iridium Hill Annex there is a negative $\delta^{13}C_{org}$ excursion of greater than 2.0‰ associated with the KPB, but no indication that $\delta^{13}C_{org}$ values trend negative prior to the Khc-Pgft as was observed in the Nirvana sections (Fig. 4A). Similarly, no overall positive trend was observed in $\delta^{13}C_{org}$ through the uppermost Khc into the lowermost Pgft portion of the section.

4.1.5. Worm Coulee

The hand trenches excavated at Worm Coulee exposed 11.2 m of section from which 42 samples were obtained, with a typical sampling resolution of 30 cm, and some more detailed sampling near the inferred Khc-Pgft contact (Fig. 5A). A sandstone layer overlies the lowermost lignite layer of the Pgft with a sharp, likely erosional contact. This sandstone has very little organic carbon, below detectable amounts in some cases, which is consistent with an interpretation of this layer as a fluvial sandstone, and likely a small disconformity exists at this point in the section. No obvious negative $\delta^{13}C_{org}$ excursion associated with the Khc-Pgft contact is observed at Worm Coulee, though there is a gradual negative trend of 0.5 to 1.0‰ over the last 2.0 m of the Khc (Fig. 5B).

4.2. Comparison of sampling methods at Nirvana

Comparison of the results of our three sampling methods (see Section 2.2) from the same hill at Nirvana (see Sections 4.1.1, 4.1.2, 4.1.3) allows us to investigate the effects of modern surficial alteration and/or contamination. We assume that the samples taken from cores are less affected by any surficial conditions than samples from either trench, though we cannot rule out the possibility that the cored material has been altered from its initial depositional condition. Broadly, all three methods show the same overall pattern in $\delta^{13}C_{org}$ over the interval where they overlap (Fig. 7A): a positive trend with a magnitude of 1.0‰ to 1.5‰, beginning about 5.0 m below the Khc-Pgft contact and ending 1.0 m above the contact. Around 1.0 m above the Khc-Pgft contact, all three sampled sections intersect a sandy layer with low total organic carbon that makes reliable $\delta^{13}C_{org}$ measurements difficult to obtain. Superimposed on this positive trend is a negative (magnitude 1.5‰ to 2.5‰) excursion beginning ~1.4 m below the Khc-Pgft contact and reaching a minimum in the IrZ coal.

However, there is a meaningful ~1.0‰ offset in $\delta^{13}C_{org}$ values between the surface samples and the cores (Fig. 7B), as demonstrated by lack of overlap between 95% prediction bounds of the LOWESS regression curves of the cores and two Nirvana trenches. The average offset between trench $\delta^{13}C_{org}$ values and the core LOWESS curve (see Section 3.3) was 0.9‰ for both trenches combined (Fig. 8A–C), which was not accompanied by a consistent or statistically significant offset in total organic carbon (Fig. 8D–F). However, there is variability in the degree of this offset (Fig. 8A,B), which may be random or driven by a cause we cannot address with our data.

4.3. Lithological control on $\delta^{13}C_{org}$

Before $\delta^{13}C_{org}$ records can be used for chemostratigraphy in regional or global frameworks, it is necessary to determine whether local changes in lithology affect $\delta^{13}C_{org}$ values (Section 3.3). Data from our sections (except for Worm Coulee) contain a negative $\delta^{13}C_{org}$ excursion near the KPB, but the minimum of that excursion occurs within the coal layer whose base defines the Khc-Pgft contact (Figs. 3B, E, 4B, 5B, 6B). A Kruskal-Wallis test on the $\delta^{13}C_{org}$ values for each section (see Section 3.3), with lithology as the predictor variable, demonstrates that lithology has a statistically significant control on $\delta^{13}C_{org}$ ($X^2 = 32.6$; $p = 1.4E-6$). Dunn-Šidák post hoc pairwise tests reveal that the $\delta^{13}C_{org}$ values from organic-rich lithologies (carbonaceous shale, lignite/coal) are statistically similar to each other, and they have significantly lower $\delta^{13}C_{org}$ values than claystone or siltstone (Fig. 9A, Table 1). Sandstone $\delta^{13}C_{org}$ values are also significantly lower than finer grained siliciclastic lithologies (i.e., claystones and siltstones). The same statistical tests applied to total organic carbon values show that lignites and carbonaceous shales have higher total organic values than other lithologies (Fig. 9B, Table 1). The correspondence between organic-rich lithologies and lower $\delta^{13}C_{org}$ values is also visually evident in the $\delta^{13}C_{org}$ records where local minima in $\delta^{13}C_{org}$ values are associated with coals and lignites, though these $\delta^{13}C_{org}$ values are not always minima for the section as whole (Figs. 3-6).

To test whether a KPB related excursion is driving the overall lower $\delta^{13}C_{org}$ values of organic lithologies, we separated KPB and non-KPB coals for statistical analysis. The mean $\delta^{13}C_{org}$ for coals and lignites associated with the KPB ($n = 6$) is higher than that for the remaining ($n = 4$) coals and lignites (Fig. 10A), but the sample sizes for both coal groupings are small, and therefore comparison tests between coals and other lithologies are not statistically significant. Because $\delta^{13}C_{org}$ values from the KPB coals are less negative than those from the non-KPB coals, KPB associated $\delta^{13}C_{org}$ values are therefore not driving the lower $\delta^{13}C_{org}$ values for the coals overall (Fig. 10A). Because all organic lithologies, including carbonaceous shales, contain similar negative excursions (Figs. 3C, F, 4C, 6C) and because carbonaceous shales have similar $\delta^{13}C_{org}$ values to coals (Fig. 9A, Table 1), we grouped these organic rich lithologies together, and then separated those associated with the KPB. This grouping provides more statistical power and demonstrates that organic-rich lithologies not associated with the KPB ($n = 14$) are distinct from other lithologies (Fig. 10B). The lower $\delta^{13}C_{org}$ value of sandstone compared with finer-grained siliciclastic rocks is still observed. Boundary organic lithologies do have lower $\delta^{13}C_{org}$ values than claystone and

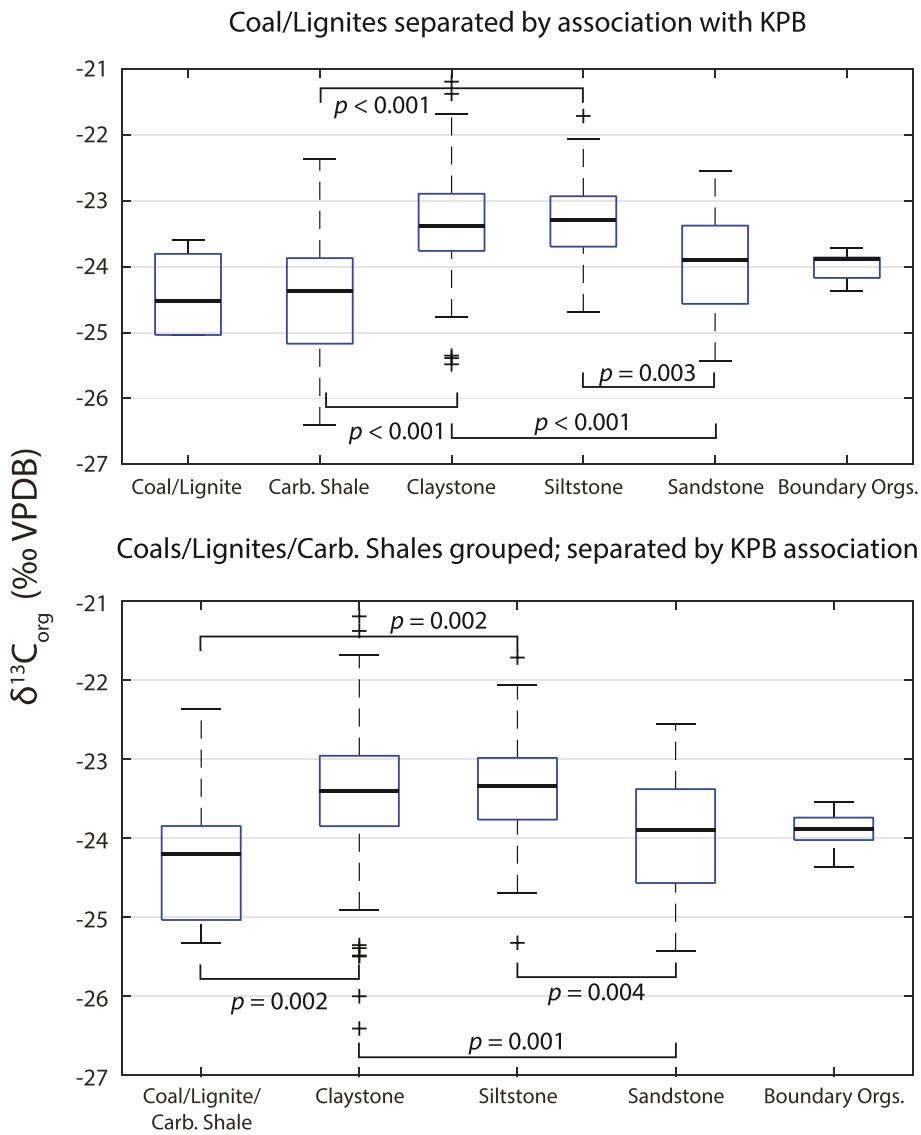

Fig. 10. Boxplots for $\delta^{13}C_{org}$ by lithology, separating boundary associated organic lithologies. These differ from Fig. 9A in that: (A) coals and lignites associated with the KPB are treated separately from other coals and lignites; (B) carbonaceous shales are grouped with coals and lignites, and those associated with the KPB are all treated separately. The *p*-values from Dunn-Šidák post hoc pairwise tests of Kruskal-Wallis test statistics are plotted for statistically significant pairwise comparisons.

siltstone, but the relationship is not statistically significant, in part due to the small number of samples ($n = 9$). The more negative $\delta^{13}C_{org}$ values of the organic rich lithologies are not due to their correspondence with the boundary.

We did not find a correlation between total organic carbon and $\delta^{13}C_{org}$ values when all of our data were evaluated together (Fig. 9C), which is similar to observations by Arens et al. (2014). This absence of correlation despite a lithological influence on $\delta^{13}C_{org}$ values implies that the environment of deposition may have a more substantial influence of $\delta^{13}C_{org}$ values than the total accumulation of organic material. Other factors, including long-term secular trends (e.g. regional vegetation shifts, atmospheric changes, etc.), may still affect $\delta^{13}C_{org}$ values. There may also be correlations between total organic carbon and $\delta^{13}C_{org}$ values over short stratigraphic windows that reveal subtle changes in deposition or even locally variable alteration of the $\delta^{13}C_{org}$ signal, and we cannot rule out additional factors that could also (or alternatively) drive local variation in $\delta^{13}C_{org}$ values.

5. Discussion

5.1. Testing modern surficial effects on $\delta^{13}C_{org}$

The offset in $\delta^{13}C_{org}$ values between trenched and cored samples (Figs. 7, 8) implies that trenched samples must have been more affected by modern surface conditions, despite efforts to recover superficially unaltered material. It is beyond the scope of this study to unequivocally determine the cause of this $\delta^{13}C_{org}$ offset, but it could result from either in situ alteration of existing organic material or contamination with modern organic carbon from several sources (or both). This alteration may occur when water from heavy rains and snowmelt follows paths made by deeply penetrating roots, which could cause oxidation of organic material and/or selective mobilization of more soluble carbon compounds at depths greater than 1 m. In the supplementary material we model the magnitude and direction of $\delta^{13}C_{org}$ offset due to modern bacterial degradation and/or contamination by modern bacterial or plant material. Alone, microbial degradation of organic matter is unlikely to explain the offset in $\delta^{13}C_{org}$ (even if microbial biomass is incorporated into the analyzed sample) largely because we observe no offset in the total organic carbon values. Contamination from modern C4

plant carbon is a more plausible explanation for our results, because it would bias the measured $\delta^{13}C_{org}$ values in the observed direction without generating large increases in organic carbon. More detailed organic chemistry will be necessary to test these hypotheses. We also do not see any evidence for mobilization of organic carbon up or down section; the point-to-point variability between the different sampling methods is similar when controlling for sampling frequency (see supplementary material).

5.2. Lithological control on $\delta^{13}C_{org}$

We see evidence for lithological correlation with $\delta^{13}C_{org}$ from our sections (see Section 4.3, Table 1, Fig. 9), which implies that different depositional environments in the continental landscape can accumulate carbon from different sources. This effect may be driven by the presence of different flora, or even different tissues from similar organisms (Bögelein et al., 2019; Graham et al., 2019). Modern fluvial environments also show depositional control on the $\delta^{13}C_{org}$, driven in part by differing contributions of autochthonous and allochthonous organic matter (Hupp et al., 2019). It is also possible that both $\delta^{13}C_{org}$ and lithology are covarying in response to global or regional environmental changes, though we are not aware of a potential causal mechanism for this response, and we consider this possibility unlikely.

Our data reveal that lithology does exert some control on $\delta^{13}C_{org}$ values, but this does not preclude $\delta^{13}C_{org}$ responding to other factors, including changes in global atmospheric CO_2. We cannot directly test the cause of this correlation, but other organic geochemical techniques, such as compound specific isotope analysis, may be capable of addressing the question. Regardless, our result contradicts previous studies, which employed both pairwise comparisons of means between different lithologies as well as the lack of correlation between total organic carbon and $\delta^{13}C_{org}$ values to argue that lithology was not a significant control on $\delta^{13}C_{org}$ in this area (Arens et al., 2014; Arens and Jahren, 2000).

5.2.1. Implications for the KPB from our data

Our data are necessarily equivocal on the validity of a KPB negative $\delta^{13}C_{org}$ excursion because none of the analyzed sections includes a definitive KPB (defined by impact ejecta) located outside of a coal layer and, locally, no sections exist that fill that criterion. We cannot be certain whether or not the short negative $\delta^{13}C_{org}$ excursions associated with the KPB were affected by global atmospheric change in addition to the local lithological change. However, much of our data is consistent with previous re-examination of North American terrestrial $\delta^{13}C_{org}$ records that found KPB-associated excursions were not unique within the analyzed sections (Grandpre et al., 2013). Notably, we see short negative excursions associated with all of the organic rich lithologies within our sections, whether or not they are associated with the KPB.

However, data from all sections at Nirvana show a more gradual trend towards more negative $\delta^{13}C_{org}$ values beginning 1.4 m below the KPB (Fig. 7), with a minimum value in the IrZ coal. This pattern is plausibly consistent with an excursion that coincides with the KPB; however, if the $\delta^{13}C_{org}$ excursion was driven by a change in the isotopic value of atmospheric carbon, that change would have begun ~50 k.y. prior to the Chicxulub bolide impact, based on typical sedimentation rates for the area (Sprain et al., 2018; Sprain et al., 2015), as the negative trend starts 1.4 m below the KPB. Because we do not see excursions beginning prior to the KPB at other published sections in the Williston Basin, we believe the most likely explanation is that the $\delta^{13}C_{org}$ data at Nirvana are capturing a localized pattern, rather than one driven by substantial changes in global atmospheric carbon (though see Section 5.2.2).

If we assume the correlation of lithology and $\delta^{13}C_{org}$ observed in our sections also holds true for other fluvial sedimentary deposits, then our results suggests that correlating continental sections using organic carbon isotopes could be challenging due to the spatial heterogeneity of depositional environments, which is particularly true for stratigraphically short excursions, especially those limited to a single bed. Spatial variability translates into stratigraphic variability, and the sequence of lithologies differs from section to section as continental environments rearrange themselves in response to channel migration and avulsion. This is true not only for correlations that involve the KPB but for any isotopic excursion that is associated with lithological change.

5.2.2. Implications for the KPB in other sections

There are three published sections in the Hell Creek area where an $\delta^{13}C_{org}$ excursion has been used to argue for the placement of the KPB separate from the local Z coal. At Hermann Ridge, Arens et al. (2014) argue that the KPB should be placed 0.9 m below the local Khc-Pgft contact due to the presence of a negative $\delta^{13}C_{org}$ excursion. This excursion is not within a coal or lignite, but it immediately follows (n = 1; 21 cm) an abrupt rise in total organic carbon (4.7%), and is located in a siltstone that has the second highest organic carbon level (1.3%) of all (n = 65) siltstones in the Hermann Ridge section, which is plausibly interpretable as a carbonaceous shale. Arens et al. (2014) also report stratigraphically shorter $\delta^{13}C_{org}$ records across the KPB from two sections 60–80 km to the east of Nirvana, at Constenius and *Z*-Line. In both cases they place the KPB 4 to 5 m below the Khc-Pgft contact based on a negative carbon isotope excursion and the stratigraphic position of an earliest Paleogene mammal fauna (Pu1) below the Khc-Pgft contact. In both sections a local $\delta^{13}C_{org}$ minimum is interpreted to indicate the KPB, but they do not report lithological descriptions of these samples. However, in both cases, these minima are from samples with very high total organic carbon values (Constenius: 8.7%; Z-line: 38.1%), sufficiently high that these layers should be interpreted as carbonaceous shales or lignites (and possibly the true Z coal), suggesting that these $\delta^{13}C_{org}$ excursions are at least in part lithologically driven. These excursions are not unique within those sections; $\delta^{13}C_{org}$ excursions of similar magnitude and duration also occur within the overlying Z coal at each locality.

In the absence of other evidence, the $\delta^{13}C_{org}$ excursions near the KPB at Hermann Ridge, Constenius, and Z-Line should not be considered independent markers for the KPB. At Constenius and Z-Line, the identified KPB may ultimately be correct, or nearly so, which is supported by the mammal biostratigraphy, but the $\delta^{13}C_{org}$ excursion may be tracking lithology, and an unrecognized Z coal, rather than global events.

Pyramid Butte in North Dakota (Arens and Jahren, 2000) is the only continental section we know of where an impact-ejecta-defined KPB is identified along with a negative $\delta^{13}C_{org}$ excursion recorded partially or entirely outside of a coal layer. In that section, a negative excursion in $\delta^{13}C_{org}$ of 1.5‰ occurs within a coal immediately below the impact claystone, and Arens and Jahren (2000) argue a separate negative 2.8‰ excursion occurs in the immediately overlying "blocky or structureless mudstone or siltstone" (Arens and Jahren, 2000; Fig. 2) which they attribute to disturbance in carbon cycling caused by the Chicxulub impact. However, detailed sample lithology and total organic carbon values are not associated with these measurements, so we cannot test whether this layer, like those at Constenius and Z-line, was also organic rich. Grandpre et al. (2013) also note that the KPB excursion at Pyramid Butte is not statistically unique in comparison to other excursions in the section.

The lower $\delta^{13}C_{org}$ values of coals and lignites that we observe does not preclude the possibility that a lithologically driven $\delta^{13}C_{org}$ change may mask an atmospheric change in $\delta^{13}C$. Due to this uncertainty, for sections where these factors cannot be decoupled, the most conservative approach is to assume that the short $\delta^{13}C_{org}$ excursion associated with the KPB is driven by local change in lithology and is not driven by a global or regional signal. It is possible that the section at Pyramid Butte does decouple these phenomena, but these types of excursions are not unique to the KPB (Grandpre et al., 2013). Without further support, we err on the side of caution and suggest that this negative shift should not be interpreted unequivocally as a response to the bolide impact, and that as such it should not be used as a chemostratigraphic marker of the KPB.

Previously published records from the area (Arens et al., 2014; Arens and Jahren, 2000; Grandpre et al., 2013; Maruoka et al., 2007) cover short temporal windows, and are therefore not capable of testing the lasting (100 s of k.y.) $\delta^{13}C$ excursion within bulk carbonate following the KPB in the marine realm. The differing durations of $\delta^{13}C_{org}$ excursions associated with the KPB in different environments has made interpreting carbon cycle disturbance difficult (Sepúlveda et al., 2019), as the apparent terrestrial $\delta^{13}C_{org}$ excursion in the Hell Creek region (Arens and Jahren, 2000) lasted less than 10 k.y. (Renne et al., 2013). We recommend against using this short $\delta^{13}C_{org}$ excursion to constrain global carbon cycling during the K-Pg extinction event unless future work can clearly separate the KPB and the $\delta^{13}C_{org}$ excursion from a carbon-rich lithology.

6. Conclusions

Modern surface weathering and/or contamination affects absolute $\delta^{13}C_{org}$ values, at least within the Khc and Pgft, and therefore absolute $\delta^{13}C_{org}$ values should be interpreted with some caution, especially when recovered from hand-dug trenches. However, the pattern and magnitude of $\delta^{13}C_{org}$ changes is largely preserved despite a roughly 1.0‰ offset towards more positive values in surface trenches, though the magnitude and direction of offset generated by surficial alteration is likely to be location specific. Interpretations that are based on understanding trends in $\delta^{13}C_{org}$ values may be valid regardless of sampling technique, and excavation or coring equipment are probably not required to sample organic carbon for these applications, though moderate trenching is still recommended, as truly surficial samples were not tested here.

The $\delta^{13}C_{org}$ records from the Hell Creek appear to be subject to some lithological control, most notably between different organic-rich lithologies and clay/siltstones. Consequently, short duration $\delta^{13}C_{org}$ changes, especially those restricted to a single stratum, from the Hell Creek region should be interpreted with caution, as these sub-meter scale shifts may be partially or entirely the result of changing lithologies. Using carbon isotope chemostratigraphy to recognize the KPB within the Hell Creek region is therefore difficult to justify. This result likely applies more broadly to continental facies at this time period, as suggested by Grandpre et al. (2013), and possibly to other time periods as well when examining short (10 k.y.) phenomena. Validating the proposed short (< 10 k.y.) KPB $\delta^{13}C_{org}$ excursion in this area requires a terrestrial stratigraphic section where the KPB is unequivocally identified (bolide impact evidence) separately from an organic-rich lithology. Pyramid Butte (Arens and Jahren, 2000) may be one such section, but the excursion at the boundary there is non-unique (Grandpre et al., 2013) and we lack the data necessary to test their section with our methods. Consequently, support for a short but profound negative carbon isotope excursion associated with the KPB is, at best, weak. The effects of the Chicxulub bolide impact are profound, but at this time currently available terrestrial carbon isotope data should not be used to constrain them.

Supplementary data to this article can be found online at https://doi.org/10.1016/j.palaeo.2021.110451.

Declaration of Competing Interest

The authors declare that they have no known competing financial interests or personal relationships that could have appeared to influence the work reported in this paper.

Acknowledgments

We acknowledge that the work presented in this paper was performed on lands that are the traditional territory of the Fort Belknap Assiniboine & Gros Ventre Tribes and Fort Peck Assiniboine & Sioux Tribes. We dedicate this paper to the memory of William A. Clemens, and thank him for advice throughout this project, and his lifelong contributions to paleontology in the Hell Creek region.

We would like the thank Dale and Jane Tharp for their hospitality, access to and through their land, equipment troubleshooting, and backhoe excavation. We additionally thank Jack Murnion for access across his land, and Greg Liggett of the Bureau of Land Management and Patrick Rennie of the Montana Department of Natural Resources and Culture for land access. We thank many people for assistance in the field, an incomplete list of which includes Ben Rodwell, Gabriella Quaresma, Gianni Aranoff, and the Discoveries in Geosciences (DIG) Field School participants Corinne Daycross and Adam Tholt. We thank Dr. Joe Lambert and the Alabama Stable Isotope Laboratory for assistance during sample analysis. We are indebted to funding for the Hell Creek Project from the Myhrvold and Havranek Charitable Family Fund. L.N.W. was supported by NSF GRFP, and L.N.W. and G.P.W.M. were supported by UW Biology and the Burke Museum. I.F. and C.S. were supported by an NSF GRFP.

References

Alvarez, L.W., 1983. Experimental evidence that an asteroid impact led to the extinction of many species 65 million years ago. Proc. Natl. Acad. Sci. U. S. A. 80, 627.

Archibald, J.D., 1982. Fossil mammalia and testudines of the Hell Creek formation, and geology of the Tullock and Hell Creek formations, Garfield Co., Montana. Univ. Calif. Publ. Earth Sci. 122, 1–286.

Archibald, J.D., Clemens, W.A., 1982. Late cretaceous extinctions: the fossil evidence currently available suggests that changes across the Cretaceous-Tertiary boundary were the result of gradual processes and not of a single catastrophic event. Am. Sci. 780, 377–385.

Archibald, J.D., Clemens, W.A., Padian, K., Rowe, T., Macleod, N., Barrett, P.M., Gale, A., Holroyd, P., Sues, H.D., Arens, N.C., Horner, J.R., Wilson, G.P., Goodwin, M.B., Brochu, C.A., Lofgren, D.L., Hurlbert, S.H., Hartman, J.H., Ebreth, D.A., Wignall, P. B., Currie, P.J., Weil, A., Prasad, G.V.R., Dingus, L., Courtillot, V., Milner, A., Milner, A., Bajpai, S., Ward, D.J., Sahni, A., 2010. Cretaceous extinctions: multiple causes. Science 328, 973.

Arens, N.C., Jahren, A.H., 2000. Carbon isotope excursion in atmospheric CO2 at the Cretaceous-Tertiary boundary: evidence from terrestrial sediments. Palaios 15, 314–322.

Arens, N.C., Jahren, A.H., 2002. Chemostratigraphic correlation of four fossil-bearing sections in southwestern North Dakota. In: The Hell Creek Formation and the Cretaceous-Tertiary Boundary in the Northern Great Plains: An Integrated Continental Record of the End of the Cretaceous. Geological Society of America. https://doi.org/10.1130/0-8137-2361-2.75.

Arens, N.C., Jahren, A.H., Kendrick, D.C., 2014. Carbon isotope stratigraphy and correlation of plant megafossil localities in the Hell Creek Formation of eastern Montana, USA. In: Geological Society of America Special Papers. Geological Society of America, pp. 149–171.

Arinobu, T., Ishiwatari, R., Kaiho, K., Lamolda, M.A., 1999. Spike of pyrosynthetic polycyclic aromatic hydrocarbons associated with an abrupt decrease in δ13C of a terrestrial biomarker at the Cretaceous-Tertiary boundary at Caravaca, Spain. Geology 27, 723–726.

Baadsgaard, H., Lerbekmo, J.F., McDougall, I., 1988. A radiometric age for the Cretaceous-Tertiary boundary based upon K-Ar, Rb-Sr, and U-Pb ages of bentonites from Alberta, Saskatchewan, and Montana. Can. J. Earth Sci. 25, 1088–1097.

Beerling, D.J., Royer, D.L., 2002. Fossil plants as indicators of the phanerozoic global carbon cycle. Annu. Rev. Earth Planet. Sci. 30, 527. https://doi.org/10.1146/annurev.earth.30.091201.141413.

Bögelein, R., Lehmann, M.M., Thomas, F.M., 2019. Differences in carbon isotope leaf-to-phloem fractionation and mixing patterns along a vertical gradient in mature European beech and Douglas fir. New Phytol. 222, 1803–1815. https://doi.org/10.1111/nph.15735.

Bourque, R.D., Douglas, P.M.J., Larsson, H.C.E., 2021. Changes in terrestrial ecosystems across the Cretaceous-Paleogene boundary in western Canada inferred from plant wax lipid distributions and isotopic measurements. Palaeogeogr. Palaeoclimatol. Palaeoecol. 562, 110081. https://doi.org/10.1016/j.palaeo.2020.110081.

Brown, R.W., 1971. Distribution of plant communities in Southeastern Montana badlands. Am. Midl. Nat. 85, 458. https://doi.org/10.2307/2423769.

Clemens, W.A., Archibald, J.D., Hickey, L.J., 1981. Out with a Whimper not a Bang. Paleobiology 7, 293–298.

Collier, A.J., Knechtel, M.M., 1939. The Coal Resources of McCone County, Montana. US Government Printing Office.

D'Hondt, S., 2005. Consequences of the cretaceous/Paleogene mass extinction for marine ecosystems. Annu. Rev. Ecol. Evol. Syst. 36, 295–317. https://doi.org/10.1146/annurev.ecolsys.35.021103.105715.

Fastovsky, D.E., 1987. Paleoenvironments of vertebrate-bearing strata during the Cretaceous-Paleogene transition, eastern Montana and western North Dakota. Palaios 282–295.

Fastovsky, D.E., Bercovici, A., 2016. The Hell Creek Formation and its contribution to the Cretaceous–Paleogene extinction: a short primer. Cretac. Res. 57, 368–390. https://doi.org/10.1016/j.cretres.2015.07.007.

Fastovsky, D.E., Dott, R.H., 1986. Sedimentology, stratigraphy, and extinctions during the Cretaceous-Paleogene transition at bug Creek, Montana. Geology 14, 279–282.
Fendley, I.M., Mittal, T., Sprain, C.J., Marvin-DiPasquale, M., Tobin, T.S., Renne, P.R., 2019. Constraints on the volume and rate of Deccan Traps flood basalt eruptions using a combination of high-resolution terrestrial mercury records and geochemical box models. Earth Planet. Sci. Lett. 524, 115721. https://doi.org/10.1016/j.epsl.2019.115721.
Gardner, A.F., Gilmour, I., 2002. Organic geochemical investigation of terrestrial Cretaceous-Tertiary boundary successions from Brownie Butte, Montana, and the Raton Basin, New Mexico. In: Catastrophic Events and Mass Extinctions: Impacts and Beyond. Geological Society of America. https://doi.org/10.1130/0-8137-2356-6.351.
Graham, H.V., Herrera, F., Jaramillo, C., Wing, S.L., Freeman, K.H., 2019. Canopy structure in Late Cretaceous and Paleocene forests as reconstructed from carbon isotope analyses of fossil leaves. Geology 47, 977–981. https://doi.org/10.1130/G46152.1.
Grandpre, R., Schauer, A., Samek, K., Veeger, A., Ward, P., Fastovsky, D., 2013. Testing the terrestrial δ13C Cretaceous–Paleogene (K–Pg) chemostratigraphic marker. Palaeogeogr. Palaeoclimatol. Palaeoecol. 381–382, 67–75. https://doi.org/10.1016/j.palaeo.2013.04.015.
Hartman, J.H., Butler, R.D., Weiler, M.W., Schumaker, K.K., 2014. Context, naming, and formal designation of the Cretaceous Hell Creek Formation lectostratotype, Garfield County, Montana. In: Geological Society of America Special Papers. Geological Society of America, pp. 89–121.
Henehan, M.J., Ridgwell, A., Thomas, E., Zhang, S., Alegret, L., Schmidt, D.N., Rae, J.W.B., Witts, J.D., Landman, N.H., Greene, S.E., Huber, B.T., Super, J.R., Planavsky, N.J., Hull, P.M., 2019. Rapid Ocean acidification and protracted Earth system recovery followed the end-cretaceous Chicxulub impact. Proc. Natl. Acad. Sci. 116, 22500–22504. https://doi.org/10.1073/pnas.1905989116.
Horner, J.R., Goodwin, M.B., Myhrvold, N., 2011. Dinosaur census reveals abundant tyrannosaurus and rare ontogenetic stages in the upper cretaceous Hell Creek formation (Maastrichtian), Montana, USA. PLoS One 6. https://doi.org/10.1371/journal.pone.0016574.
Hull, P.M., Bornemann, A., Penman, D.E., Henehan, M.J., Norris, R.D., Wilson, P.A., Blum, P., Alegret, L., Batenburg, S.J., Bown, P.R., Bralower, T.J., Cournede, C., Deutsch, A., Donner, B., Friedrich, O., Jehle, S., Kim, H., Kroon, D., Lippert, P.C., Loroch, D., Moebius, I., Moriya, K., Peppe, D.J., Ravizza, G.E., Röhl, U., Schueth, J.D., Sepúlveda, J., Sexton, P.F., Sibert, E.C., Śliwińska, K.K., Summons, R.E., Thomas, E., Westerhold, T., Whiteside, J.H., Yamaguchi, T., Zachos, J.C., 2020. On impact and volcanism across the Cretaceous-Paleogene boundary. Science 367, 266–272. https://doi.org/10.1126/science.aay5055.
Hupp, C.R., Kroes, D.E., Noe, G.B., Schenk, E.R., Day, R.H., 2019. Sediment trapping and carbon sequestration in floodplains of the lower Atchafalaya Basin, LA: allochthonous versus autochthonous carbon sources. J. Geophys. Res. Biogeosci. 124, 663–677. https://doi.org/10.1029/2018JG004533.
Ickert, R.B., Mulcahy, S.R., Sprain, C.J., Banaszak, J.F., Renne, P.R., 2015. Chemical and Pb isotope composition of phenocrysts from bentonites constrains the chronostratigraphy around the Cretaceous-Paleogene boundary in the Hell Creek region, Montana. Geochem. Geophys. Geosyst. 16, 2743–2761. https://doi.org/10.1002/2015GC005898.
Keller, G., Lindinger, M., 1989. Stable isotope, TOC and CaCO3 record across the cretaceous/tertiary boundary at El Kef, Tunisia. Palaeogeogr. Palaeoclimatol. Palaeoecol. 73, 243–265. https://doi.org/10.1016/0031-0182(89)90007-2.
Landman, N.H., Goolaerts, S., Jagt, J.W.M., Jagt-Yazykova, E.A., Machalski, M., Yacobucci, M.M., 2014. Ammonite extinction and nautilid survival at the end of the cretaceous. Geology 42, 707–710. https://doi.org/10.1130/G35776.1.
Lofgren, D.L., 1995. The Bug Creek Problem and the Cretaceous-Tertiary Transition at McGuire Creek. Univ of California Press, Montana.
Longrich, N.R., Bhullar, B.-A.S., Gauthier, J.A., 2012. Mass extinction of lizards and snakes at the Cretaceous-Paleogene boundary. Proc. Natl. Acad. Sci. 109, 21396–21401. https://doi.org/10.1073/pnas.1211526110.
Maruoka, T., Koeberl, C., Bohor, B.F., 2007. Carbon isotopic compositions of organic matter across continental Cretaceous–Tertiary (K–T) boundary sections: Implications for paleoenvironment after the K–T impact event. Earth Planet. Sci. Lett. 253, 226–238. https://doi.org/10.1016/j.epsl.2006.10.028.
Milligan, J.N., Royer, D.L., Franks, P.J., Upchurch, G.R., McKee, M.L., 2019. No evidence for a large atmospheric CO2 spike across the Cretaceous-Paleogene boundary. Geophys. Res. Lett. 46, 3462–3472. https://doi.org/10.1029/2018GL081215.
Moore, J.R., Wilson, G.P., Sharma, M., Hallock, H.R., Braman, D.R., 2014. Assessing the relationships of the Hell Creek–Fort Union contact, Cretaceous-Paleogene boundary, and Chicxulub impact ejecta horizon at the Hell Creek Formation lectostratotype, Montana, US. Geol. Soc. Am. Spec. Pap. 503, 123–136.
Morgan, M.E., Kingston, J.D., Marino, B.D., 1994. Carbon isotopic evidence for the emergence of C4 plants in the Neogene from Pakistan and Kenya. Nature 367, 162–165. https://doi.org/10.1038/367162a0.
Noorbergen, L.J., Abels, H.A., Hilgen, F.J., Robson, B.E., de Jong, E., Dekkers, M.J., Krijgsman, W., Smit, J., Collinson, M.E., Kuiper, K.F., 2018. Conceptual models for short-eccentricity-scale climate control on peat formation in a lower Palaeocene fluvial system, North-Eastern Montana (USA). Sedimentology 65, 775–808. https://doi.org/10.1111/sed.12405.
Renne, P.R., Deino, A.L., Hilgen, F.J., Kuiper, K.F., Mark, D.F., Mitchell, W.S., Morgan, L.E., Mundil, R., Smit, J., 2013. Time scales of critical events around the Cretaceous-Paleogene boundary. Science 339, 684–687. https://doi.org/10.1126/science.1230492.
Saltzman, M.R., Thomas, E., 2012. Carbon isotope stratigraphy. In: The Geologic Time Scale. Elsevier, pp. 207–232.
Scannella, J.B., Fowler, D.W., Goodwin, M.B., Horner, J.R., 2014. Evolutionary trends in Triceratops from the Hell Creek formation, Montana. Proc. Natl. Acad. Sci. 111, 10245–10250. https://doi.org/10.1073/pnas.1313334111.
Schenk, H.J., Jackson, R.B., 2002. Rooting depths, lateral root spreads and below-ground/above-ground allometries of plants in water-limited ecosystems. J. Ecol. 90, 480–494. https://doi.org/10.1046/j.1365-2745.2002.00682.x.
Schimmelmann, A., DeNiro, M.J., 1984. Elemental and stable isotope variations of organic matter from a terrestrial sequence containing the cretaceous/Tertiary boundary at York Canyon, New Mexico. Earth Planet. Sci. Lett. 68, 392–398. https://doi.org/10.1016/0012-821X(84)90124-9.
Schulte, P., Alegret, L., Arenillas, I., Arz, J.A., Barton, P.J., Bown, P.R., Bralower, T.J., Christeson, G.L., Claeys, P., Cockell, C.S., Collins, G.S., Deutsch, A., Goldin, T.J., Goto, K., Grajales-Nishimura, J.M., Grieve, R.A.F., Gulick, S.P.S., Johnson, K.R., Kiessling, W., Koeberl, C., Kring, D.A., MacLeod, K.G., Matsui, T., Melosh, J., Montanari, A., Morgan, J.V., Neal, C.R., Nichols, D.J., Norris, R.D., Pierazzo, E., Ravizza, G., Rebolledo-Vieyra, M., Reimold, W.U., Robin, E., Salge, T., Speijer, R.P., Sweet, A.R., Urrutia-Fucugauchi, J., Vajda, V., Whalen, M.T., Willumsen, P.S., 2010. The Chicxulub asteroid impact and mass extinction at the Cretaceous-Paleogene boundary. Science 327, 1214–1218. https://doi.org/10.1126/science.1177265.
Sepúlveda, J., Alegret, L., Thomas, E., Haddad, E., Cao, C., Summons, R.E., 2019. Stable isotope constraints on marine productivity across the Cretaceous-Paleogene mass extinction. Paleoceanogr. Paleoclimatol. 34, 1195–1217. https://doi.org/10.1029/2018PA003442.
Shure, L., 2011. Data Driven Fitting. https://blogs.mathworks.com/loren/2011/01/13/data-driven-fitting/ (accessed 2.17.21).
Smit, J., Van Der Kaars, S., 1984. Terminal cretaceous extinctions in the Hell Creek area, Montana: compatible with catastrophic extinction. Science 223, 1177–1179.
Smith, S.M., Sprain, C.J., Clemens, W.A., Lofgren, D.L., Renne, P.R., Wilson, G.P., 2018. Early mammalian recovery after the end-cretaceous mass extinction: a high-resolution view from McGuire Creek area, Montana, USA. GSA Bull. https://doi.org/10.1130/B31926.1.
Sprain, C.J., Renne, P.R., Wilson, G.P., Clemens, W.A., 2015. High-resolution chronostratigraphy of the terrestrial Cretaceous-Paleogene transition and recovery interval in the Hell Creek region, Montana. Geol. Soc. Am. Bull. 127, 393–409. https://doi.org/10.1130/B31076.1.
Sprain, C.J., Renne, P.R., Clemens, W.A., Wilson, G.P., 2018. Calibration of chron C29r: New high-precision geochronologic and paleomagnetic constraints from the Hell Creek region, Montana. GSA Bull. https://doi.org/10.1130/B31890.1.
Swisher III, C.C., Dingus, L., Butler, R.F., 1993. ^{40}Ar/ ^{39}Ar dating and magnetostratigraphic correlation of the terrestrial Cretaceous–Paleogene boundary and Puercan Mammal Age, Hell Creek – Tullock formations, eastern Montana. Can. J. Earth Sci. 30, 1981–1996. https://doi.org/10.1139/e93-174.
The Mathworks, Inc, 2020. Statistics and Machine Learning Toolbox. Natick, MA, USA.
Therrien, F., Eberth, D.A., Braman, D.R., Zelenitsky, D.K., 2007. High-resolution organic carbon isotope record across the Cretaceous–Tertiary boundary in south- central Alberta: implications for the post-impact recovery rate of terrestrial ecosystems and use of δ13C as a boundary marker. Can. J. Earth Sci. 44, 14.
Tipple, B.J., Pagani, M., Krishnan, S., Dirghangi, S.S., Galeotti, S., Agnini, C., Giusberti, L., Rio, D., 2011. Coupled high-resolution marine and terrestrial records of carbon and hydrologic cycles variations during the Paleocene–Eocene thermal Maximum (PETM). Earth Planet. Sci. Lett. 311, 82–92. https://doi.org/10.1016/j.epsl.2011.08.045.
Tobin, T.S., Wilson, G.P., Eiler, J.M., Hartman, J.H., 2014. Environmental change across a terrestrial Cretaceous-Paleogene boundary section in eastern Montana, USA, constrained by carbonate clumped isotope paleothermometry. Geology 42, 351–354. https://doi.org/10.1130/G35262.1.
Wilson, G.P., 2005. Mammalian faunal dynamics during the last 1.8 million years of the cretaceous in Garfield County, Montana. J. Mamm. Evol. 12, 53–76.
Wilson, G.P., 2013. Mammals across the K/Pg boundary in northeastern Montana, U.S.A.: dental morphology and body-size patterns reveal extinction selectivity and immigrant-fueled ecospace filling. Paleobiology 39, 429–469. https://doi.org/10.1666/12041.
Wilson, G.P., 2014. Mammalian extinction, survival, and recovery dynamics across the Cretaceous-Paleogene boundary in northeastern Montana, U.S.A. Geol. Soc. Am. Spec. Pap. 503, 365–390.